Paper 151

Proceedings of the Eleventh International Conference
on Computational Structures Technology,
B.H.V. Topping, (Editor),
Civil-Comp Press, Stirlingshire, Scotland

Structural Response of a Composite Beam subject to Cyclic Loading Conditions considering the Interfacial Slip Effect

J.W. Hwang, H.G. Kwak and Y.H. Lee
Department of Civil and Environmental Engineering
KAIST, Daejeon, Republic of Korea

Abstract

An extension of a model, which can simulate the bond-slip effect at the interface between the slab and the girder of composite beams, in cyclic loading condition is introduced. The model is based on non-linear finite element (FE) method adopting a simple beam element for which the nodal degree of freedom is only two (one lateral deflection and one rotation) even without taking a double node. Hysteresis models of concrete and steel are adopted to implement cyclic stress-strain relations. An incremental approach to replicate the non-linear cyclic shear behaviour of shear connectors and a unique iteration method searching double neutral axis are also proposed. The performance of the model is verified by comparing the analysis results by the model with experimental results for a simply supported composite beam structure under cyclic load.

Keywords: bond-slip, beam element, cyclic loading, hysteresis model, composite beam, shear connector, non-linear analysis.

1 Introduction

Composite structures are generally constructed by placing slab concrete on steel or pre-cast concrete girders to achieve the monolithic behaviour of a structure with shear connectors. The structural behaviour of the composite member becomes more complicated due to different material properties of slab and girder. Bond-slip is usually present along the interface of the composite beams and, the slip behaviour becomes growingly clear with the increase of the external load. Thus, when the structural response is in not only elastic range but also inelastic range, where severe loadings such as fully reversed cyclic loadings are applied, it is necessary to evaluate the structural behaviour with the slip effect.

A finite element based model [1], which can consider bond-slip effect at the interface without adopting the double-node concept under arbitrary loadings, is extended to be applied into even cyclic lateral loadings and the model is applied to

analyze a steel-concrete composite beam in this paper. In the analysis, cyclic load-slip relation of shear connectors and hysteresis models of concrete and steel are considered to replicate the cyclic material behaviour and, structural response for the composite beam through the application of the model are compared with existing experimental results to verify the performance of the proposed model.

2 Material Models

2.1 Concrete

Among the numerous mathematical models currently used in the analysis of RC structures, the monotonic envelop curve introduced by Kent and Park [2] and later extended by Scott et al. [3] is adopted in this paper because of its simplicity and computational efficiency. For the hysteretic behaviour of concrete in compressive region, simplified model by Karsan and Jirsa [4] is adopted as shown in Fig. 1(a) and hysteretic stress-strain behaviour in the tensile region is according to Fig. 1(b). All the details and application of the monotonic and cyclic model can be found elsewhere [1, 5].

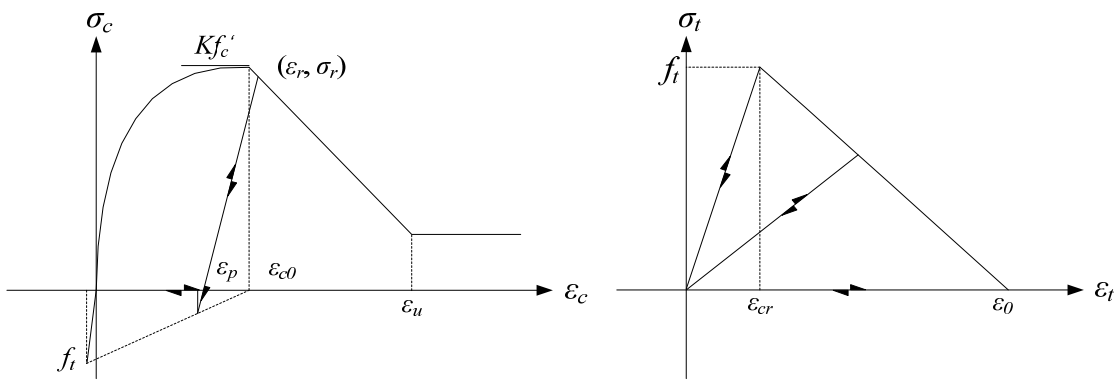

(a) Compressive region (b) Tensile region

Fig. 1. Hysteretic stress-strain relation of concrete

2.2 Steel

The monotonic envelope of stress-strain relationship of steel was idealized as elasto-plastic behaviour and the shape of the curve is assumed to be identical in the both of compressive and tensile area. Among a number of models developed to describe the cyclic stress–strain curve of steel, the most commonly used approach is the Giuffre-Menegotto–Pinto model [6, 7], and it is also adopted in this paper as shown in Fig. 2. Detailed equations and application of the cyclic steel model can be also found elsewhere [5].

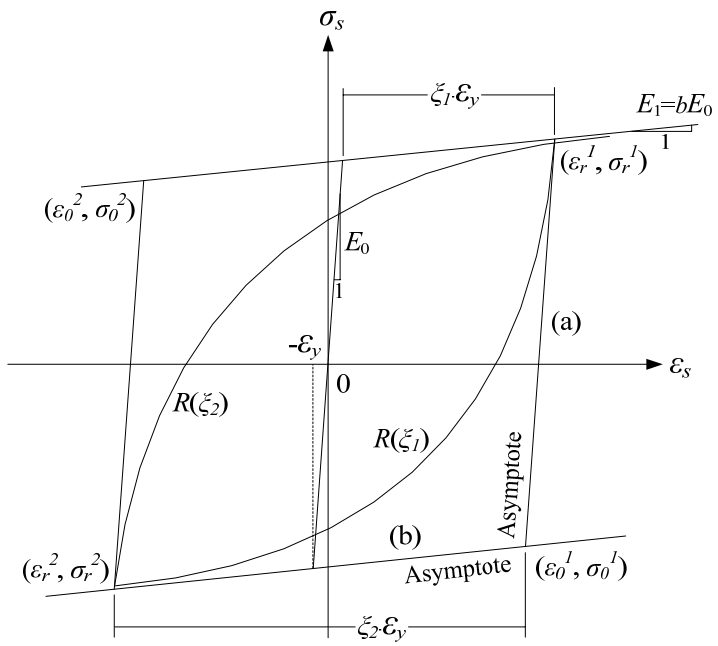

Fig. 2. Hysteretic stress-strain curve of steel

3 Slip Evaluation

3.1 Load-slip Relation

Since composite beams are equipped with shear connectors between a concrete slab and girder to unify the behaviour of the total structure, the flexural and slip behaviour of these composite beams are greatly influenced by the shear connectors, which are characterized by load-slip relation. Many tests have been performed to investigate the mechanical behaviour of shear connectors under monotonic and cyclic loadings experimentally and material constitutive models for shear connectors have been also proposed on the basis of the experimental results. Among them, Salari proposed a bond constitutive law which expresses effectively behaviour of shear studs under cyclic shear loadings [8], and in this paper this model is adopted as the load-slip relation. In this model, the monotonic envelope is divided into two parts of ascending and descending branches at the shear strength V_1 in Fig. 3, and each part can be defined by Eqs. (1) and (2), respectively:

$$V = V_1 \alpha_1 \frac{S}{S_1} Exp\left(-\alpha_2 \left(\frac{S}{S_1} \right)^{\alpha_3} \right), \quad \left(0 \le S \le S_1 \right) \tag{1}$$

$$V = V_1 \beta_1 Exp\left(-\beta_2 \left(\frac{S}{S_1} - 1 \right)^{\beta_3} \right) + V_{fu}, \quad \left(S_1 < S \right), \tag{2}$$

where V_{fu} is the ultimate frictional resistance, $\alpha_1 = K_0/K_1$, $\alpha_2 = -Ln(1/\alpha_1)$, $\alpha_3 = 1/\alpha_2$,

$\beta_1 = 1 - \overline{V}_{fu}$, $\beta_2 = -(Ln(R_2))/(\overline{S}_2 - 1)^{\beta_3}$,

$\beta_3 = \left(Ln\left(\frac{Ln(R_2)}{Ln(R_3)} \right) \right) \Big/ \left(Ln\left(\frac{\overline{S}_2 - 1}{\overline{S}_3 - 1} \right) \right)$, $R_i = (\overline{V}_i - \overline{V}_{fu})/(1 - \overline{V}_{fu})$, $\overline{V}_{fu} = V_{fu}/V_1$, $\overline{V}_i = V_i/V_1$,

$\overline{S}_i = S_i/S_1$, and i =2, 3.

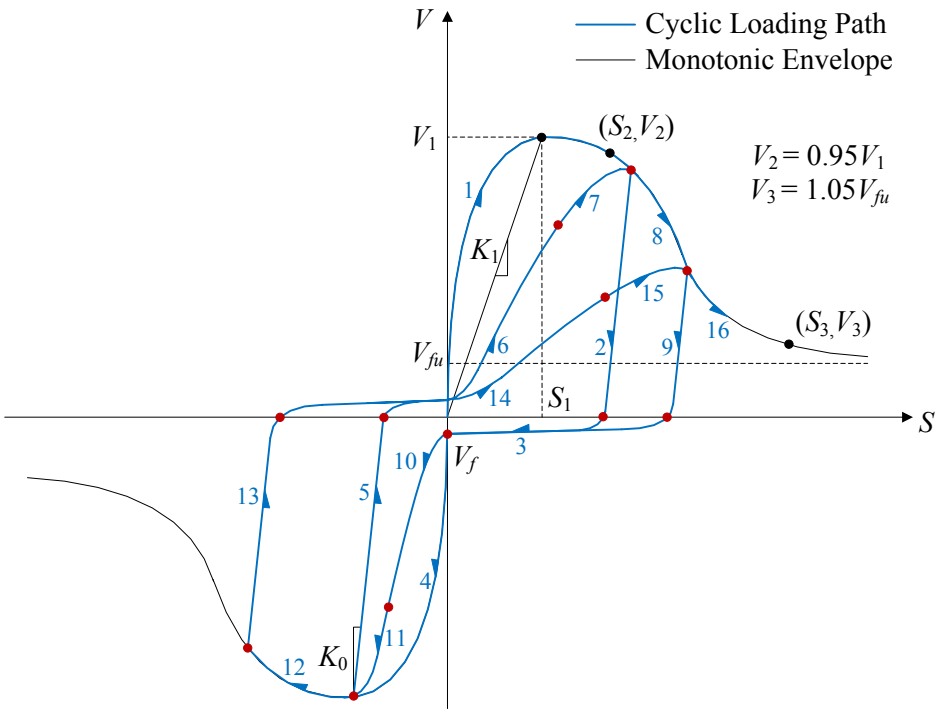

Fig. 3. Cyclic load-slip relation of shear connectors

In case of cyclic behaviour, when unloading arises at first, the loading path is divided into two segments. It drops with its initial stiffness K_0. Then it undergoes non-linear transition in exponential form and meets slip axis in the 1st segment (path 2 in Fig. 3). In the 2nd segment, the path moves to frictional resistance (0, V_f) in form of cubic function until it meets monotonic envelope (path 3 in Fig. 3) in the opposite side. When unloading arises in the opposite side, the loading path is divided into three segments (paths 5, 6 & 7 in Fig. 3). Differently with the first unloading pattern, 2nd segment on the path 6 continues after it meets monotonic envelope in the opposite side and the degradation in stiffness arises at that moment. Also, 3rd unloading segment expressed as the second order Bezier curve is added from second unloading (path 7 in Fig. 3). The other unloading paths in the Fig. 3 follow the same pattern which is divided into 3 segments. Reloading path has 2 segments that are similar with the 2nd & 3rd segments in unloading behaviour and all the details of these patterns and equations are defined elsewhere [8].

3.2 Incremental Approach for the Non-linearity

If shear connectors are assumed to be installed under the uniform spacing L_s and the load-slip curve of a shear connector is linear, the slip S can be represented by the following Eq. (3), where $q(x)$ is the shear force transmitted per unit length of the beam known as the shear flow ($q(x) = dF/dx$). F is horizontal force in coordinate x at the interface between two materials, which will be explained in the next chapter in detail, and K_s is stiffness of load-slip relation.

$$S = \frac{V(x)}{K_S} = \frac{q(x)L_S}{K_S} \tag{3}$$

However, if shear connectors behave non-linearly, the stiffness K_s becomes variable changed according to slip value S and the value is expressed by following Eqs. (4) and (5), obtained by differentiating the load V (Eqs. (1) and (2)) by slip S (only monotonic envelope is mentioned here).

$$K(S) = \frac{dV}{dS} = \alpha_1 \cdot \left|\frac{V_1}{S_1}\right| \cdot \left\{1 - \alpha_2\alpha_3\left(\left|\frac{S}{S_1}\right|\right)^{\alpha_3}\right\} \cdot Exp\left\{-\alpha_2\left(\left|\frac{S}{S_1}\right|\right)^{\alpha_3}\right\}, \quad (0 \le S \le S_1) \tag{4}$$

$$K(S) = \frac{dV}{dS} = -\beta_1\beta_2\beta_3 \cdot \left|\frac{V_1}{S_1}\right| \cdot \left(\left|\frac{S}{S_1}\right| - 1\right)^{\beta_3 - 1} \cdot Exp\left\{-\beta_2\left(\left|\frac{S}{S_1}\right| - 1\right)^{\beta_3}\right\}, \quad (S_1 < S) \tag{5}$$

Then, total slip S can be evaluated approximately by accumulating all the slip change (S^j) values like Eqs. (6) and (7) where superscription j and m mean the considered load step number and the number of total load steps in the FE analysis respectively.

$$S = \sum_{j=1}^{m} S^j \tag{6}$$

$$S^j = \frac{V^j(x)}{K_s} = \frac{q^j(x) \cdot L_S}{K(S^{j-1})} \tag{7}$$

3.3 Governing Equation of Slip Behaviour

The governing equation of slip behaviour is induced from substituting the static equilibrium of internal force in axial direction and strain relationship by the classical beam theory at the interface into the slip constitutive law $\varepsilon_{slip} = dS/dx = \varepsilon_{b,top} - \varepsilon_{s,bottom}$ where subscript s and b mean upper slab and lower beam (girder) respectively. The obtained governing equation is expressed as Eq. (8) and detailed derivation procedures can be found elsewhere [1].

$$\frac{d^2F(x)_{horz.}}{dx^2} - \frac{K_s}{L_s}\frac{EI^*}{EA^*\sum EI}F(x)_{horz.} = -\frac{K_s}{L_s}\frac{(h_b+h_s)}{(E_bI_b+E_sI_s)}M(x) \tag{8}$$

In the Eq. (8), E is modulus of material, A is section area, h is centroidal distance from the interface for each own component, I is inertia moment of section, $1/EA^* = 1/E_sA_s + 1/E_bA_b$, $EI^* = \Sigma EI + EA^*\cdot(h_s + h_b)^2$ and $F_{horz.}$ is horizontal force increment applied along the material interface at coordinate x in an element at a load step. Section rigidity values EA, EA^*, EI and EI^* can be computed by summation of all values for layers in the layered section approach. For computational convenience, the differential equation in Eq. (8) can be rewritten in the form of $F''(x) - P^2F(x) = -QM(x)$ and, $F(x)$, the general solution of Eq. (1), is obtained by summing a particular solution to the associated homogeneous solution, and the corresponding distribution of slip increment $S(x)$ is also obtained from Eq. (7). These lead to

$$\begin{Bmatrix} F_i(x) \\ S_i(x) \end{Bmatrix} = \begin{bmatrix} cosh(P_ix) & sinh(P_ix) \\ T_i\,sinh(P_ix) & T_i\,cosh(P_ix) \end{bmatrix} \begin{Bmatrix} \alpha_i \\ \beta_i \end{Bmatrix} + \frac{Q_i}{P_i^2}\begin{Bmatrix} M_i(x) \\ \frac{L_{s,i}}{K_{s,i}}D_i \end{Bmatrix} \tag{9}$$

where $D(x)$ means the slope of the incremental moment distribution and α & β are unknown coefficients of each subdivided element.

3.4 Numerical Slip Model

When boundary conditions at the two far ends of the simply supported beam, horizontal force & moment should be zero, and continuity conditions of slip and horizontal force increment at the boundary of each element are applied into Eq. (9) sequentially for the all elements, following system matrix equation (Eq. 10) can be obtained [1]:

$$\begin{Bmatrix} 0 \\ f(S^{n+1}) \end{Bmatrix} = \begin{bmatrix} G_{11} & G_{12} \\ G_{21} & G_{22} \end{bmatrix} \begin{Bmatrix} 0 \\ f(S^1) \end{Bmatrix} + \begin{Bmatrix} H_1 \\ H_2 \end{Bmatrix} \tag{10}$$

and it can be simplified like

$$\mathbf{D}_n = \mathbf{G}\mathbf{D}_1 + \mathbf{H} \tag{11}$$

where $\mathbf{G} = \prod_{i=1}^{n}\mathbf{Z}_i = \mathbf{Z}_n\cdot\mathbf{Z}_{n-1}\cdot\cdots\cdot\mathbf{Z}_2\cdot\mathbf{Z}_1$, $\mathbf{H} = \sum_{i=2}^{n}\left\{\left[\prod_{j=i}^{n}\mathbf{Z}_j\right]\Delta\mathbf{M}_i\right\}$, $\Delta\mathbf{M}_i = \mathbf{M}_{i-1} - \mathbf{M}_i$

$$\mathbf{Z}_i = \mathbf{C}_{1,i}\mathbf{C}_{2,i}^{-1}, \mathbf{A}_i = \begin{Bmatrix} \alpha_i \\ \beta_i \end{Bmatrix}, \ \mathbf{A}_{i-1} = \begin{Bmatrix} \alpha_{i-1} \\ \beta_{i-1} \end{Bmatrix}, \ \mathbf{M}_{i-1} = \frac{Q_{i-1}}{P_{i-1}^2} \begin{Bmatrix} M^i \\ \frac{L_{s,i-1}}{K_{s,i-1}} D_{i-1} \end{Bmatrix},$$

$$\mathbf{M}_i = \frac{Q_i}{P_i^2} \begin{Bmatrix} M^i \\ \frac{L_{s,i}}{K_{s,i}} D_i \end{Bmatrix}, \ \mathbf{C}_{1,i-1} = \begin{bmatrix} cosh(P_{i-1}\frac{l_{i-1}}{2}) & sinh(P_{i-1}\frac{l_{i-1}}{2}) \\ T_{i-1}\,sinh(P_{i-1}\frac{l_{i-1}}{2}) & T_{i-1}\,cosh(P_{i-1}\frac{l_{i-1}}{2}) \end{bmatrix} \text{ and}$$

$$\mathbf{C}_{2,i}^{-1} = \begin{bmatrix} cosh(-P_i\frac{l_i}{2}) & sinh(-P_i\frac{l_i}{2}) \\ T_i\,sinh(-P_i\frac{l_i}{2}) & T_i\,cosh(-P_i\frac{l_i}{2}) \end{bmatrix}^{-1} = \begin{bmatrix} cosh(P_i\frac{l_i}{2}) & \frac{1}{T_i}sinh(P_i\frac{l_i}{2}) \\ sinh(P_i\frac{l_i}{2}) & \frac{1}{T_i}cosh(P_i\frac{l_i}{2}) \end{bmatrix}. \tag{12}$$

Solving simultaneous equation composed of 2 rows of 2 X 2 system matrix equation (Eq. 11) yields the slip values at the two far ends (S^1 and S^{n+1}) of the structure. When two nodal slip values are obtained, the solution coefficient α and β can be computed in sequential manner according to Table. 1 and detailed procedures can be found elsewhere [1].

The formulations can be applied also in the case where the two far ends are not simply supported. The changes are only in the matrices $\mathbf{D}_1$ and $\mathbf{D}_n$ in Eq. (11) because only these matrices include the terms such as F^1, F^{n+1}, M^1, M^{n+1}, S^1 and S^{n+1} dependent on the boundary conditions. If the support is fixed end, horizontal force and moment at the boundary has some values and, on the other hand, slip is zero by the restriction of the fixed end. Then, the unknown for the fixed end is not the nodal slip S^1 but F^1 unlike the simply supported end. All the changes in formulation according to the boundary conditions are arranged in the Table. 1.

When the slip model is applied to the non-linear problem, where stiffness of stud K_s is changed according to slip value, all the procedures can be repeated for every load step and, total slip value should be computed by accumulating all the incremental values as mentioned in chapter 3.2. If the path enters into the descending branch in the accumulating process, where the stiffness K_s is negative value, a slight modification for the solution procedure is required because P^2 becomes negative value and hyperbolic function in Eq. (9) includes a meaningless imaginary number P. Thus, when the path is on the descending branch, the governing differential equation should be changed into $F''(x) + P^2F(x) = -QM(x)$ where $P^2 = -\frac{K_s}{L_s}\frac{EI^*}{EA^*\sum EI}$. All the related remaining solution procedures are similar with those for the loading path on the ascending branch [1] and also arranged in Table. 1.

ASCENDING BRANCH ($K_S > 0$)	DESCENDING BRANCH ($K_S < 0$)
Horizontal force and slip distributions	
$F(x) = F_h + F_p = \alpha\, cosh(Px) + \beta\, sinh(Px) + \frac{Q}{P^2} M(x)$	$F(x) = F_h + F_p = \alpha\, cos(Px) + \beta\, sin(Px) - \frac{Q}{P^2} M(x)$
$S(x) = \frac{L_s}{K_s}\left\{\alpha P\, sinh(Px) + \beta P\, cosh(Px) + \frac{Q}{P^2} D(x)\right\}$	$S(x) = \frac{L_s}{K_s}\left\{-\alpha P\, sin(Px) + \beta P\, cos(Px) - \frac{Q}{P^2} D(x)\right\}$
$\begin{Bmatrix} F_i(x) \\ S_i(x) \end{Bmatrix} = \begin{bmatrix} cosh(P_i x) & sinh(P_i x) \\ T_i\, sinh(P_i x) & T_i\, cosh(P_i x) \end{bmatrix} \begin{Bmatrix} \alpha_i \\ \beta_i \end{Bmatrix} + \frac{Q_i}{P_i^2} \begin{Bmatrix} M_i(x) \\ \frac{L_{s,i}}{K_{s,i}} D_i \end{Bmatrix}$	$\begin{Bmatrix} F_i(x) \\ S_i(x) \end{Bmatrix} = \begin{bmatrix} cos(P_i x) & sin(P_i x) \\ -T_i\, sin(P_i x) & T_i\, cos(P_i x) \end{bmatrix} \begin{Bmatrix} \alpha_i \\ \beta_i \end{Bmatrix} - \frac{Q_i}{P_i^2} \begin{Bmatrix} M_i(x) \\ \frac{L_{s,i}}{K_{s,i}} D_i \end{Bmatrix}$
Applying compatibility conditions for continuity into Eq. (9)	
$F^i = F_{i-1}\left(\frac{l_{i-1}}{2}\right) = F_i\left(-\frac{l_i}{2}\right),\ S^i = S_{i-1}\left(\frac{l_{i-1}}{2}\right) = S_i\left(-\frac{l_i}{2}\right)$	
$\mathbf{A}_i = \mathbf{C}_{2,i}^{-1}\mathbf{C}_{1,i-1}\mathbf{A}_{i-1} + \mathbf{C}_{2,i}^{-1}\left[\mathbf{M}_{i-1} - \mathbf{M}_i\right] = \mathbf{C}_{2,i}^{-1}\mathbf{C}_{1,i-1}\mathbf{A}_{i-1} + \mathbf{C}_{2,i}^{-1}\Delta\mathbf{M}_i$, where $\mathbf{A}_i = \begin{Bmatrix} \alpha_i \\ \beta_i \end{Bmatrix},\ \mathbf{A}_{i-1} = \begin{Bmatrix} \alpha_{i-1} \\ \beta_{i-1} \end{Bmatrix}$, $\mathbf{M}_{i-1} = \frac{Q_{i-1}}{P_{i-1}^2}\begin{Bmatrix} M^i \\ \frac{L_{s,i-1}}{K_{s,i-1}} D_{i-1} \end{Bmatrix},\ \mathbf{M}_i = \frac{Q_i}{P_i^2}\begin{Bmatrix} M^i \\ \frac{L_{s,i}}{K_{s,i}} D_i \end{Bmatrix}$, $\mathbf{C}_{1,i-1} = \begin{bmatrix} cosh(P_{i-1}\frac{l_{i-1}}{2}) & sinh(P_{i-1}\frac{l_{i-1}}{2}) \\ T_{i-1}\, sinh(P_{i-1}\frac{l_{i-1}}{2}) & T_{i-1}\, cosh(P_{i-1}\frac{l_{i-1}}{2}) \end{bmatrix}$, $\mathbf{C}_{2,i}^{-1} = \begin{bmatrix} cosh(-P_i\frac{l_i}{2}) & sinh(-P_i\frac{l_i}{2}) \\ T_i\, sinh(-P_i\frac{l_i}{2}) & T_i\, cosh(-P_i\frac{l_i}{2}) \end{bmatrix}^{-1} = \begin{bmatrix} cosh(P_i\frac{l_i}{2}) & \frac{1}{T_i} sinh(P_i\frac{l_i}{2}) \\ sinh(P_i\frac{l_i}{2}) & \frac{1}{T_i} cosh(P_i\frac{l_i}{2}) \end{bmatrix}$	$\mathbf{A}_i = \mathbf{C}_{2,i}^{-1}\mathbf{C}_{1,i-1}\mathbf{A}_{i-1} + \mathbf{C}_{2,i}^{-1}\left[\mathbf{M}_{i-1} - \mathbf{M}_i\right] = \mathbf{C}_{2,i}^{-1}\mathbf{C}_{1,i-1}\mathbf{A}_{i-1} + \mathbf{C}_{2,i}^{-1}\Delta\mathbf{M}_i$, where $\mathbf{A}_i = \begin{Bmatrix} \alpha_i \\ \beta_i \end{Bmatrix},\ \mathbf{A}_{i-1} = \begin{Bmatrix} \alpha_{i-1} \\ \beta_{i-1} \end{Bmatrix}$, $\mathbf{M}_{i-1} = -\frac{Q_{i-1}}{P_{i-1}^2}\begin{Bmatrix} M^i \\ \frac{L_{s,i-1}}{K_{s,i-1}} D_{i-1} \end{Bmatrix},\ \mathbf{M}_i = -\frac{Q_i}{P_i^2}\begin{Bmatrix} M^i \\ \frac{L_{s,i}}{K_{s,i}} D_i \end{Bmatrix}$, $\mathbf{C}_{1,i-1} = \begin{bmatrix} cos(P_{i-1}\frac{l_{i-1}}{2}) & sin(P_{i-1}\frac{l_{i-1}}{2}) \\ -T_{i-1}\, sin(P_{i-1}\frac{l_{i-1}}{2}) & T_{i-1}\, cos(P_{i-1}\frac{l_{i-1}}{2}) \end{bmatrix}$, $\mathbf{C}_{2,i}^{-1} = \begin{bmatrix} cos(-P_i\frac{l_i}{2}) & sin(-P_i\frac{l_i}{2}) \\ -T_i\, sin(-P_i\frac{l_i}{2}) & T_i\, cos(-P_i\frac{l_i}{2}) \end{bmatrix}^{-1} = \begin{bmatrix} cos(P_i\frac{l_i}{2}) & \frac{1}{T_i} sin(P_i\frac{l_i}{2}) \\ -sin(P_i\frac{l_i}{2}) & \frac{1}{T_i} cos(P_i\frac{l_i}{2}) \end{bmatrix}$
Applying boundary conditions into Eq. (9)	
Case I: Simply supported	Case I: Simply supported
$\mathbf{A}_1 = \begin{Bmatrix} \alpha_1 \\ \beta_1 \end{Bmatrix} = \mathbf{C}_{2,1}^{-1}\mathbf{D}_1 = \mathbf{C}_{2,1}^{-1}\begin{Bmatrix} 0 \\ S^1 - \frac{L_{s,1}}{K_{s,1}}\frac{Q_1}{P_1^2} D_1 \end{Bmatrix} = \mathbf{C}_{2,1}^{-1}\begin{Bmatrix} 0 \\ f(S^1) \end{Bmatrix}$	$\mathbf{A}_1 = \begin{Bmatrix} \alpha_1 \\ \beta_1 \end{Bmatrix} = \mathbf{C}_{2,1}^{-1}\mathbf{D}_1 = \mathbf{C}_{2,1}^{-1}\begin{Bmatrix} 0 \\ S^1 + \frac{L_{s,1}}{K_{s,1}}\frac{Q_1}{P_1^2} D_1 \end{Bmatrix} = \mathbf{C}_{2,1}^{-1}\begin{Bmatrix} 0 \\ f(S^1) \end{Bmatrix}$
$\mathbf{A}_n = \begin{Bmatrix} \alpha_n \\ \beta_n \end{Bmatrix} = \mathbf{C}_{1,n}^{-1}\mathbf{D}_n = \mathbf{C}_{1,n}^{-1}\begin{Bmatrix} 0 \\ S^{n+1} - \frac{L_{s,n}}{K_{s,n}}\frac{Q_n}{P_n^2} D_n \end{Bmatrix} = \mathbf{C}_{1,n}^{-1}\begin{Bmatrix} 0 \\ f(S^{n+1}) \end{Bmatrix}$	$\mathbf{A}_n = \begin{Bmatrix} \alpha_n \\ \beta_n \end{Bmatrix} = \mathbf{C}_{1,n}^{-1}\mathbf{D}_n = \mathbf{C}_{1,n}^{-1}\begin{Bmatrix} 0 \\ S^{n+1} + \frac{L_{s,n}}{K_{s,n}}\frac{Q_n}{P_n^2} D_n \end{Bmatrix} = \mathbf{C}_{1,n}^{-1}\begin{Bmatrix} 0 \\ f(S^{n+1}) \end{Bmatrix}$
Case II: Cantilever or propped cantilever	Case II: Cantilever or propped cantilever
$\mathbf{A}_1 = \begin{Bmatrix} \alpha_1 \\ \beta_1 \end{Bmatrix} = \mathbf{C}_{2,1}^{-1}\mathbf{D}_1 = \mathbf{C}_{2,1}^{-1}\begin{Bmatrix} F^1 - \frac{Q_1}{P_1^2} M^1 \\ -\frac{L_{S,1}}{K_{S,1}}\frac{Q_1}{P_1^2} D_1 \end{Bmatrix}$	$\mathbf{A}_1 = \begin{Bmatrix} \alpha_1 \\ \beta_1 \end{Bmatrix} = \mathbf{C}_{2,1}^{-1}\mathbf{D}_1 = \mathbf{C}_{2,1}^{-1}\begin{Bmatrix} F^1 + \frac{Q_1}{P_1^2} M^1 \\ \frac{L_{S,1}}{K_{S,1}}\frac{Q_1}{P_1^2} D_1 \end{Bmatrix}$
$\mathbf{A}_n = \begin{Bmatrix} \alpha_n \\ \beta_n \end{Bmatrix} = \mathbf{C}_{1,n}^{-1}\mathbf{D}_n = \mathbf{C}_{1,n}^{-1}\begin{Bmatrix} 0 \\ S^{n+1} - \frac{L_{S,n}}{K_{S,n}}\frac{Q_n}{P_n^2} D_n \end{Bmatrix}$	$\mathbf{A}_n = \begin{Bmatrix} \alpha_n \\ \beta_n \end{Bmatrix} = \mathbf{C}_{1,n}^{-1}\mathbf{D}_n = \mathbf{C}_{1,n}^{-1}\begin{Bmatrix} 0 \\ S^{n+1} + \frac{L_{S,n}}{K_{S,n}}\frac{Q_n}{P_n^2} D_n \end{Bmatrix}$
Case III: Two fixed ends	Case III: Two fixed ends
$\mathbf{A}_1 = \begin{Bmatrix} \alpha_1 \\ \beta_1 \end{Bmatrix} = \mathbf{C}_{2,1}^{-1}\mathbf{D}_1 = \mathbf{C}_{2,1}^{-1}\begin{Bmatrix} F^1 - \frac{Q_1}{P_1^2} M^1 \\ -\frac{L_{S,1}}{K_{S,1}}\frac{Q_1}{P_1^2} D_1 \end{Bmatrix}$	$\mathbf{A}_1 = \begin{Bmatrix} \alpha_1 \\ \beta_1 \end{Bmatrix} = \mathbf{C}_{2,1}^{-1}\mathbf{D}_1 = \mathbf{C}_{2,1}^{-1}\begin{Bmatrix} F^1 + \frac{Q_1}{P_1^2} M^1 \\ \frac{L_{S,1}}{K_{S,1}}\frac{Q_1}{P_1^2} D_1 \end{Bmatrix}$
$\mathbf{A}_n = \begin{Bmatrix} \alpha_n \\ \beta_n \end{Bmatrix} = \mathbf{C}_{1,n}^{-1}\mathbf{D}_n = \mathbf{C}_{1,n}^{-1}\begin{Bmatrix} F^{n+1} - \frac{Q_n}{P_n^2} M^{n+1} \\ -\frac{L_{S,n}}{K_{S,n}}\frac{Q_n}{P_n^2} D_n \end{Bmatrix}$	$\mathbf{A}_n = \begin{Bmatrix} \alpha_n \\ \beta_n \end{Bmatrix} = \mathbf{C}_{1,n}^{-1}\mathbf{D}_n = \mathbf{C}_{1,n}^{-1}\begin{Bmatrix} F^{n+1} + \frac{Q_n}{P_n^2} M^{n+1} \\ \frac{L_{S,n}}{K_{S,n}}\frac{Q_n}{P_n^2} D_n \end{Bmatrix}$

Table. 1. Slip analysis formulations for ascending and descending branches

4 FE Analysis Procedures

FE analysis procedures in this paper is based on the beam element of which degrees of freedom is four, one lateral deflection and one rotation at each node in an element, and all the constitutive equations are formulated by the assumption of Timoshenko beam. Details related to the derivation procedure can be found elsewhere [1] and a unique iteration method for the convergence proposed in this paper, different from the conventional one, is the focus of this chapter.

At the early stage of the first load step, the section analysis is performed based on the status of the full connection between the layer in the slab and the one in the girder, which is assumed in the conventional layered section method (see Fig. 4). When the analysis procedures converge, the early stage ends. Right after the early stage ends, bond slip analysis begins. Here, the slip analysis procedures mentioned in the previous chapter need to be re-arranged appropriately to be unity with the discrete element system of a FE analysis unlike the solution steps to solve the governing equation. The procedures can be summarized as follows dividing steps by the main variables that should be obtained in the slip analysis.

(1) Coefficients of the governing equation (P_i, Q_i and $M_i(x)$) are computed.
(2) 2 nodal unknown values (among S^1, S^{n+1}, F^1 and F^{n+1}) at two far ends are computed.
(3) Solution coefficients α_i and β_i of each element are computed.
(4) The horizontal force $F_{horz.}$ and slip S of each element are computed.
(5) The strain and stress distributions of the section of each element is transformed into the discontinuous ones.
(6) The convergence is checked and iteration performed.

In the step (5), continuous strain distribution resulted in the early stage, where a full connection is assumed, is transformed into discontinuous one determined by the slip effect. Although there are no additional changes of the external forces, this discontinuous strain distribution induces residual forces in the structure. Thus, the strain should be re-distributed by the additional iteration loop until the convergence criteria is satisfied, which is referred to the late analysis stage of the 1st load step, and it is the step (6).

In the step (6), the criteria condition in the section analysis level is changed differently with the early stage because the horizontal force, induced by the consideration of the slip effect, is applied at the material interface. In the early stage, the only sufficient condition is that the summation of internal axial force values of all layers should be within assumed tolerance value in the process of bi-sectional repetitive strategy finding a single neutral axis of the section by the assumption of a full connection. However, a different criteria condition, that the summation of internal axial force in both of two components should be same with the value of horizontal force at the interface, is required in the late analysis stage. So, in the late analysis stage, two neutral axis values of each component should be found to satisfy two criteria conditions, the equilibrium of the horizontal force of each component (the slab and the girder) and, bi-sectional repetitive strategy is applied for two

components in the parallel process to obtain both of two neutral axis values(see Fig. 4).

When the 2nd load increment is applied to the structure, bi-sectional repetitive strategy to find double neutral axis starts again assuming that the horizontal force value obtained in the last iteration step of the 1st load increment is kept with the change of curvature induced by the 2nd load increment (1st iteration step). Then, step (1)~(4) are performed to obtain horizontal force and slip distributions and, the residual forces in the 1st iteration step of the 2nd load increment are applied to the structure as the external loads. Thereafter, step (6) and step (1)~(4) repeats changing the criteria conditions by updated horizontal force values until the convergence is ensured. The analysis procedures in an arbitrary ith load increment next to the 2nd load increment are same with the one in the 2nd load increment and following Fig. 4 shows iteration strategy in load-deflection curve including interfacial bond-slip effect compared with conventional FE iteration steps assuming a full connection.

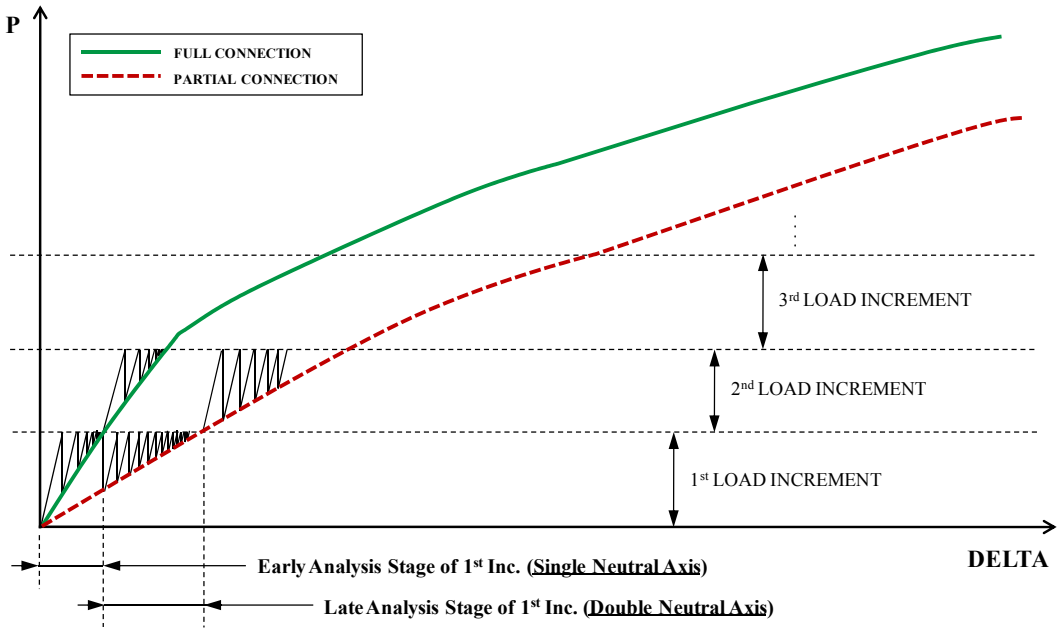

Fig. 4. Comparison of the proposed iteration strategy with conventional one

5 Analysis & Verification

For the verification of applicability of the proposed slip analysis method under cyclic loading conditions, a steel composite beam is analyzed and comparison between analysis results and actual experimental results is performed. The example is composite beam C3 by Takanashi et al. [9] and, in the experiment, fully steel composite beam was tested. Thus, the comparison is performed between fully connected experimental results and analysis results assuming the full connection and, the differences with the partial connection considering the slip effect are investigated also in this example. A concrete slab, of which breadth & height were 1000mm &

65mm, was cast on the top flange of the steel beam and, web thickness, flange thickness, total depth and flange breadth of steel beam were 5.8mm, 6.5mm, 202.9mm and 101.6mm each other. For reinforcing of the slab, steel bars of which diameter were 6mm were latticed at a depth of 17mm from the slab surface with 100mm spacing. The structure, of which total length was 2.9m, was simply supported and the load was applied at the mid-span cyclically. Material properties of the composite beam quoted in this paper to compare analysis results with are arranged in the Table. 2. For the shear studs, material properties are assumed appropriately so that the mechanical behaviours of shear stud, like un-loading, re-loading branches and frictional slip zone, mentioned in the chapter 3.1, can reflected into the analysis well.

Concrete Strength (MPa)	Steel Strength		Shear Stud		
	Girder (MPa)	Reinforcement (MPa)	Initial Stiffness (kN/mm)	Strength (kN)	Stud Distance (mm)
20.03	333.0	570.0	300.0	50.0	300.0

Table. 2. Material properties of the steel composite beam C3

Fig. 5 shows the analysis results assuming the full connection at the interface compared with experiments of fully composite beam C3. The x-axis means the normalized rotation value, evaluated by dividing mid-span deflection by span length, with ${}_s\theta_p$ which is defined as ${}_sM_p/3EI$ (${}_sM_p$ is the full plastic moments of steel beam, 55.89kN·m, and EI is the flexural rigidity) and y-axis means normalized bending moment at the mid-span by the full plastic moments of composite beam, ${}_cM_p$, of which values are 106.82kN·m in the positive moment section and 69.57kN·m in the negative moment section. In the Fig. 5, analysis results show an excellent agreement with experiment for whole cycles. On the other hand, analysis results considering the bond-slip effect in Fig. 6 make differences with analysis and experiment with the full connection. In the unloading paths, the curve representing the analysis results considering the slip shows a pretty high flexible structural response, compared with experiment provided a full connection, typically observed in partially composite beams and, in the reloading paths, the moment capacity is decreased clearly in the positive moment quadrants. These phenomena are caused by the slip effect and become more remarkable as the slip changes are enlarged in the frictional slip zone.

6 Conclusion

A slip model based on the finite element method is extended in this paper. The model can consider the interfacial bond-slip effect even without inserting substantial degrees of freedom in the axial direction. The model is improved so that composite beams under cyclic lateral loading conditions can be analysed adopting non-linear approach of the behaviour of shear studs under cyclic shear loadings and hysteresis models of concrete and steel. The analysis results by the model are compared with experimental results to verify the performance of the model. The model replicates the structural behaviour considering the interfacial slip very well and shows very appropriate cyclic path movements.

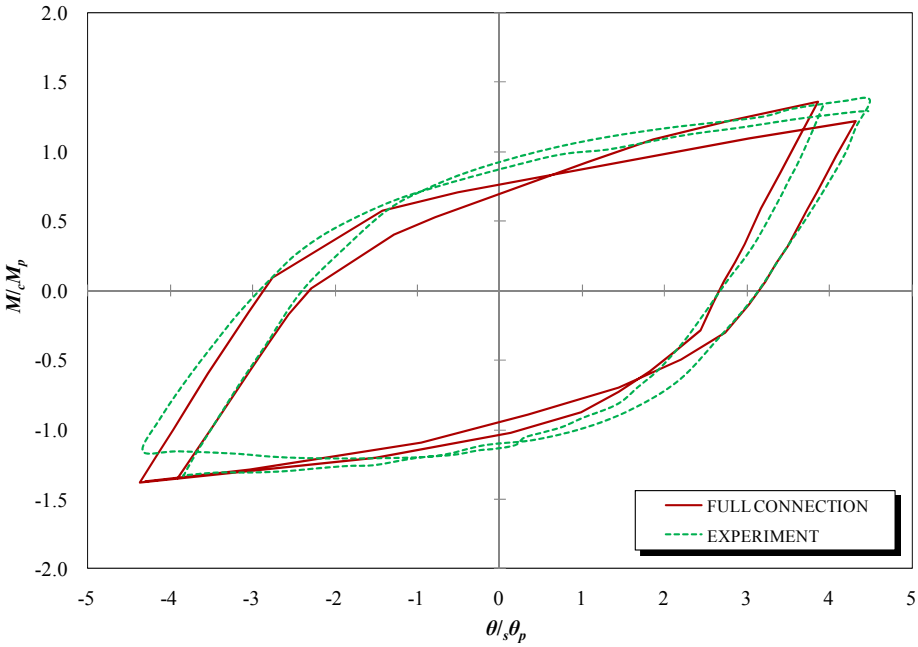

Fig. 5. Rotation-moment curve for the example assuming full connection

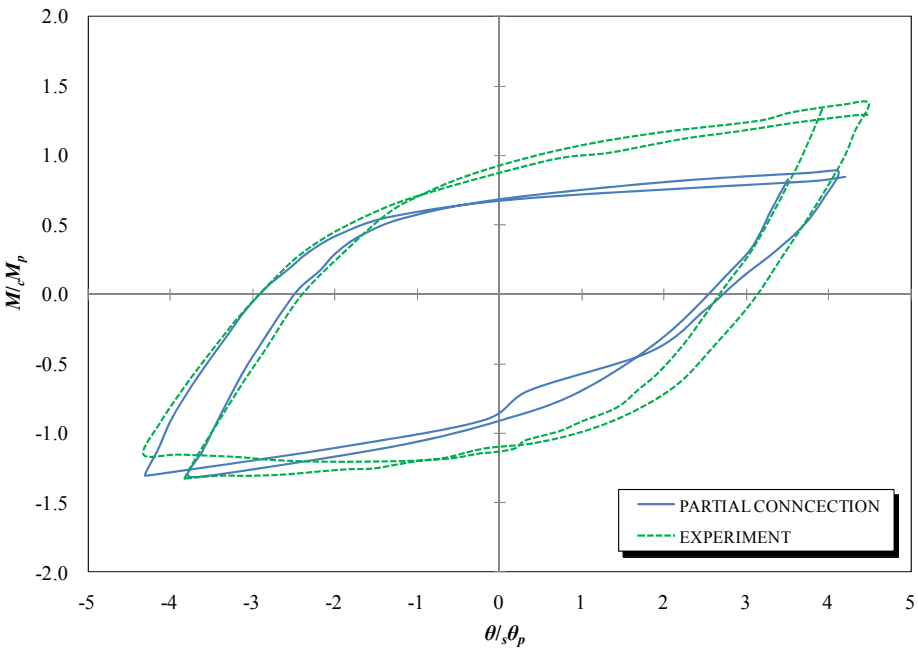

Fig. 6. Rotation-moment curve for the example considering bond-slip effect

Acknowledgement

This research was financially supported by U-city Master and Doctor Course Grant Program and a grant (07High Tech A01) from High tech Urban Development Program funded by Ministry of Land, Transportation and Maritime Affairs of Korean government.

References

[1] H.G. Kwak, J.W. Hwang, "FE model to simulate bond-slip behavior in composite concrete beam bridges", Computers and Structures, 88(17-18), 973-984, 2010.

[2] D.C. Kent, R. Park, "Flexural members with confined concrete", ASCE Journal of Structural Division, 97(5), 1969-1990, 1971.

[3] B.D. Scott, R. Park, M.J.N. Priestley, "Stress–strain behavior of concrete confined by overlapping hoops at low and high strain rates", ACI Structural Journal, 79(1), 13–27, 1982.

[4] I.D. Karsan, J.O. Jirsa, "Behavior of concrete under compressive loadings", ASCE Journal of the Structural Division, 95(12), 2543-2563, 1969.

[5] H.G. Kwak, J.K. Kim, "Implementation of bond-slip effect in analysis of RC frames under cyclic loads using layered section method", Engineering Structures, 28(12), 1715-1727, 1999.

[6] A. Giuffre, P. Pinto, "Il comportamento del cemento armato per sollecitazioni cicliche di forte intensita", Giornale del Genio Civile, 5, 391-408, 1970.

[7] M. Menegotto, P. Pinto, "Method of analysis for cyclically loaded reinforced concrete plane frames including changes in geometry and nonelastic behavior of elements under combined normal force and bending", in "Proceedings of IABSE Symposium on Resistance and Ultimate Deformability of Structures acted on by well defined repeated loads", Lisbon, Portugal, 1973.

[8] M.R. Salari, "Modeling of bond-slip in steel-concrete composite beams and reinforcing bars", University of Colorado, 1999.

[9] K. Takanashi, K. Usagawa, "Behaviors of steel and composite beams at various displacement rates", ASCE Journal of Structural Engineering, 115(8), 2067-2081, 1989.